Chemistry Research Journal, 2020, 5(6):37-58

Available online www.chemrj.org

Research Article

ISSN: 2455-8990
CODEN(USA): CRJHA5

A DFT Investigation of the Relationships between Electronic Structure and D_2, 5-HT_{1A}, 5-HT_{2A}, 5-HT_6 and 5-HT_7 Receptor Affinities in a group of Fananserin derivatives

Juan S. Gómez-Jeria, Valentina Rojas-Candia

Quantum Pharmacology Unit, Department of Chemistry, Faculty of Sciences, University of Chile. Las Palmeras 3425, Santiago 7800003, Chile.
Corresponding author: facien03@uchile.cl

Abstract The Klopman-Peradejordi-Gómez QSAR method was employed to find relationships between electronic structure and receptor affinity in a series of Fananserin derivatives. We analyzed the affinities for D_2, 5-HT_{1A}, 5-HT_{2A}, 5-HT_6 and 5-HT_7 receptors. The electronic structure was calculated at the DFT B3LYP/6-31G(d,p) level. For all cases a statistically significant equation was obtained explaining the variation of the affinity in terms of the variation of the numerical values of a set of local atomic reactivity indices. All equations show that sigma electrons of the saturated carbon chain and the saturated ring seem to play an important role in the regulation of the receptor affinity. Several kinds of atom-atom interactions are suggested. From the results the corresponding 2D pharmacophores were built.

Keywords Fananserin, QSAR, Dopamine, Serotonin, Klopman-Peradejordi-Gómez method, structure-activity relationships, electronic structure, chemical reactivity, pharmacophore

Introduction

Dopamine (DA) is a small molecule acting as a hormone and a neurotransmitter that plays several important roles in the brain and body. DA constitutes nearly 80% of the catecholamine content in the brain. Dysfunctions of the dopamine system are associated with many neurological and psychiatric disorders [1-6]. Serotonin is also a small molecule acting as a neurotransmitter modulating cognition, learning, memory, mood, reward and many physiological processes such as vomiting and vasoconstriction [7]. Both molecules act at several receptor subtypes. Dopamine binds to receptors called D_1 to D_5 and serotonin to 5-HT_{1A}, 5-HT_{1B}, 5-HT_{1D}, 5-HT_{1E}, 5-HT_{1F}, 5-HT_{2A}, 5-HT_{2B}, 5-HT_{2C}, 5-HT_3, 5-HT_4, 5-HT_{5A}, 5-HT_{5B}, 5-HT_6 and 5-HT_7 receptors. Some exogenous molecules such as amphetamine, mescaline, hallucinogenic amphetamines, LSD, bufotenin and DMT also bind to these receptors.

There are many families of large synthetic compounds presenting affinity for several dopamine and serotonin receptors at the same time [8-15]. What still needs to be elucidated in these large molecules is the knowledge about which part or parts of them play a role in regulating their affinity for these various receptors and which part or parts of them regulate the different biological responses produced by these unions. In out Unit we have carried out many theoretical studies of structure-activity relationships in several families of drugs binding to serotonin [16-23] and dopamine [24-29] receptors.

Recently a series of Fananserin derivatives was synthesized and tested for their affinity for various dopamine and serotonin receptors [11]. Fananserin acts as a potent antagonist at both the 5-HT_{2A} receptor and the dopamine D_4 receptor but it does not block the dopamine D_2 receptor. In this paper we present the results of the application of the Klopman-Peradejordi-Gómez (KPG) method for obtaining formal relationships between electronic structure and receptor affinity of these fananserin derivatives.

Methods, Models and Calculations

The selected molecules are a group of Fananserin derivatives selected from a recent study [11]. Their general formula and biological activities are displayed, respectively, in Fig. 1 and Table 1.

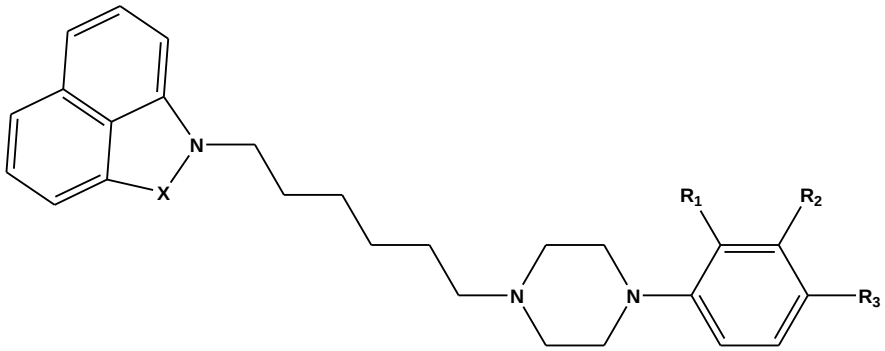

Figure 1: General formula of Fananserin derivatives

Table 1: Fananserin derivatives and receptor binding affinities[11].

Mol.	X	R_1	R_2	R_3	$\log(K_i)$ D_2	$\log(K_i)$ 5-HT_{1A}	$\log(K_i)$ 5-HT_{2A}	$\log(K_i)$ 5-HT_6	$\log(K_i)$ 5-HT_7
1	SO_2	F	H	H	1.95	1.91	2.58	2.85	2.31
2	SO_2	Cl	H	H	2.15	2.03	2.74	2.71	2.46
3	SO_2	H	Cl	H	2.08	1.66	2.51	2.80	2.64
4	SO_2	H	H	Cl	2.53	2.29	2.25	2.64	2.45
5	SO_2	Cl	Cl	H	2.34	2.17	2.17	2.37	2.15
6	SO_2	H	Cl	Cl	2.40	1.90	2.40	2.35	2.61
7	SO_2	H	CF_3	H	2.48	2.12	2.78	2.57	2.22
8	SO_2	H	H	CF_3	2.97	3.00	3.18	2.97	3.78
9	C=O	F	H	H	2.51	1.81	2.72	3.24	2.62
10	C=O	Cl	H	H	1.76	1.82	2.73	3.23	2.53
11	C=O	H	Cl	H	1.88	1.63	2.63	2.68	1.72
12	C=O	H	H	Cl	2.29	2.26	2.63	2.84	2.09
13	C=O	Cl	Cl	H	1.97	2.09	2.61	2.96	3.71
14	C=O	H	Cl	Cl	2.39	2.21	2.69	3.27	2.22
15	C=O	H	H	Br	2.31	2.84	3.17	3.50	3.26
16	C=O	CF_3	H	H	2.21	2.78	3.25	3.05	4.25
17	C=O	H	CF_3	H	2.70	1.73	2.89	3.35	2.46
18	C=O	H	H	CF_3	2.98	2.73	3.64	3.31	4.69

The Klopman-Peradejordi-Gómez (KPG) method is a linear equation relating any kind of biological activity with a set of local atomic reactivity indices. For its development we refer the reader to the literature [30-41]. During all the years of its use it has produced excellent results for a wide variety of molecules and biological activities [16, 17, 20, 22, 25, 26, 29, 42-67].

The electronic structure was calculated within the Density Functional Theory (DFT) at the B3LYP/6-31g(d,p) level after full geometry optimization [68]. The Gaussian suite of programs was used [69]. To calculate the numerical values of the local atomic reactivity indices weemployed data from the Gaussian results. The D-Cent-QSAR software was employed [70]. All the electron populations smaller than or equal to 0.01 e were considered as zero [35]. Negative electron populations coming from Mulliken Population Analysis were corrected as usual [71]. Because the resolution of the system of linear equations is not possible because we have not enough molecules, we made use of Linear Multiple Regression Analysis (LMRA) techniques to find the best solution. For each case, a matrix containing the dependent variable (the biological activity of each case and the local atomic reactivity indices of all atoms of the common skeleton as independent variables was built. The Statistica software was used for LMRA [72].

We worked with the common skeleton hypothesis stating that there is a definite collection of atoms, common to all molecules analyzed, that accounts for nearly all the biological activity [34]. The action of the substituents consists in modifying the electronic structure of the common skeleton and influencing the right alignment of the drug throughout the orientational parameters. It is hypothesized that different parts or this common skeleton accounts for almost all the interactions leading to the expression of a given biological activity. The common skeleton is shown in Fig. 2.

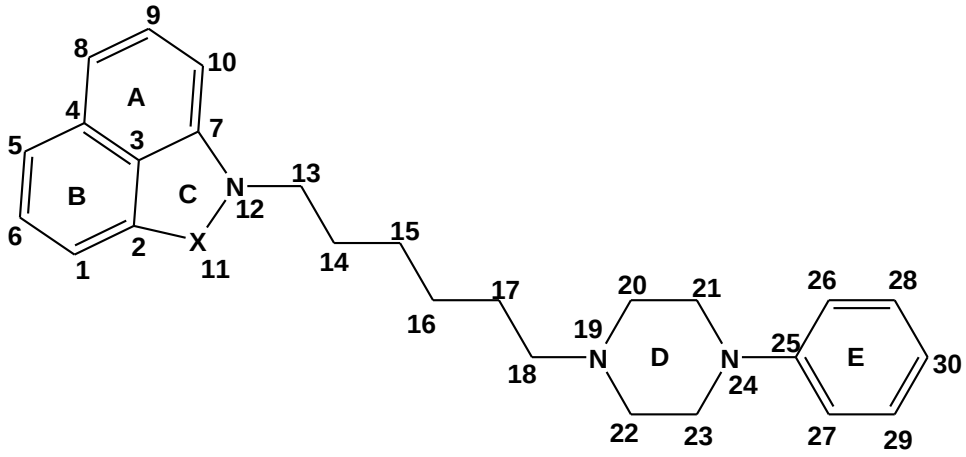

Figure 2: Common skeleton numbering

Results

Results for 5-HT$_{1A}$ receptor binding affinity

The best equation obtained is:

$$\log(K_i) = 1.96 - 0.57S_8^{E}(\mathrm{HOMO}-1)^* - 1.38S_{14}^{N}(\mathrm{LUMO})^* + 0.009S_{21}^{N} - \\ -1.30S_{21}^{E}(\mathrm{HOMO}-1)^* - 0.42F_{26}(\mathrm{LUMO}+2)^* \quad (1)$$

with n=18, R=0.98, R^2=0.96, adj-R^2=0.95, F(5,12)=65.42 ($p<0.000001$) and SD=0.09. No outliers were detected and no residuals fall outside the ±2σ limits. Here, S_8^{E}(HOMO-1)* is the electrophilic superdelocalizability of the second highest occupied local MO of atom 8, S_{14}^{N}(LUMO)* is the nucleophilic superdelocalizability of the highest empty local MO of atom 12, S_{21}^{N} is the total atomic nucleophilic superdelocalizability of atom 21, S_{21}^{E}(HOMO-1)* is the electrophilic superdelocalizability of the second highest occupied local MO of atom 21 and F_{26}(LUMO+2)* is the Fukui index of the third lowest empty local MO of atom 26.Tables 2 and 3 show, respectively, the beta coefficients, the results of the t-test for significance of coefficients and the matrix of squared correlation coefficients for the variables of Eq. 1. There are no significant internal correlations between independent variables (Table 3). Figure 3 displays the plot of observed vs. calculated log(K_i).

Table 2: Beta coefficients and t-test for significance of coefficients in Eq. 1.

	Beta	t(12)	p-level
S_8^E(HOMO-1)*	-0.77	-12.38	<0.000000
S_{14}^N(LUMO)*	-0.60	-10.38	<0.000000
S_{21}^N	0.33	5.68	0.0001
S_{21}^E(HOMO-1)*	-0.33	-5.60	0.0001
F_{26}(LUMO+2)*	-0.26	-4.53	0.0007

Table 3: Matrix of squared correlation coefficients for the variables in Eq. 1.

	S_8^E(HOMO-1)*	S_{14}^N(LUMO)*	S_{21}^N	S_{21}^E(HOMO-1)*
S_{14}^N(LUMO)*	0.10	1.00		
S_{21}^N	0.07	0.01	1.00	
S_{21}^E(HOMO-1)*	0.04	0.01	0.04	1.00
F_{26}(LUMO+2)*	0.03	0.02	0.00	0.03

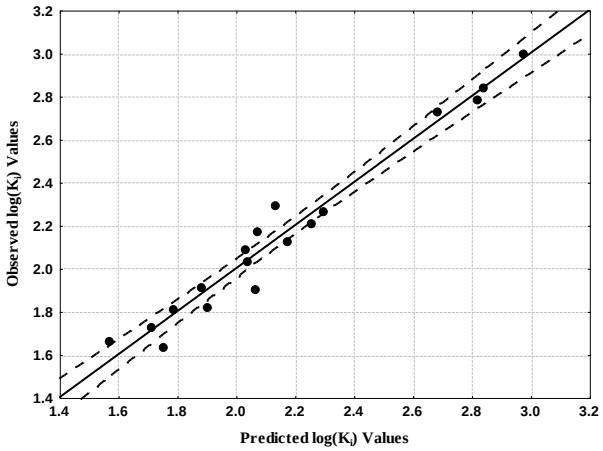

Figure 3: Plot of predicted vs. observed log(K_i) values (Eq. 1). Dashed lines denote the 95% confidence interval

The associated statistical parameters of Eq. 1 indicate that this equation is statistically significant and that the variation of the numerical values of a group of five local atomic reactivity indices of atoms of the common skeleton explains about 95% of the variation of the 5-HT_{1A} receptor affinity. Figure 3, spanning about 1.4 orders of magnitude, shows that there is a good correlation of observed *versus* calculated values.

Results for 5-HT_{2A} receptor binding affinity

The best equation obtained is:

$$\log(K_i) = 3.47 - 0.32S_8^{\,E}\left(\mathrm{HOMO}-1\right)^* - 1.82F_{30}\left(\mathrm{LUMO}+1\right)^* - \\ -0.86S_{21}^{\,N}\left(\mathrm{LUMO}+2\right)^* - 0.16\mu_{16}^* - 0.71S_{16}^{\,N}\left(\mathrm{LUMO}+2\right)^* \quad (2)$$

with n=18, R=0.97, R^2=0.95, adj-R^2=0.93, F(5,12)=44.21 (p<0.000001) and SD=0.10. No outliers were detected and no residuals fall outside the ±2σ limits. Here, S_8^E(HOMO-1)* is the electrophilic superdelocalizability of the second highest occupied local MO of atom 8, F_{30}(LUMO+1)* is the Fukui index of the second lowest empty local MO of atom 30, S_{21}^N(LUMO+2)* is the nucleophilic superdelocalizability of the third lowest empty local MO of atom 21, μ_{16}^* is the local electronic chemical potential of atom 16 and S_{16}^N(LUMO+2)* is the nucleophilic superdelocalizability of the third lowest local MO of atom 16.Tables 4 and 5 show the beta coefficients, the results of the t-test for significance of coefficients and the matrix of squared correlation coefficients for the variables of Eq.

2. There are no significant internal correlations between independent variables (Table 5). Figure 4 displays the plot of observed vs. calculated $\log(K_i)$.

Table 4: Beta coefficients and t-test for significance of coefficients in Eq. 2

	Beta	t(12)	p-level
S_8^E(HOMO-1)*	-0.49	-7.02	0.00001
F_{30}(LUMO+1)*	-0.55	-7.25	0.00001
S_{21}^N(LUMO+2)*	-0.40	-5.66	0.0001
μ_{16}^*	-0.36	-4.86	0.0004
S_{16}^N(LUMO+2)*	-0.21	-3.02	0.01

Table 5: Matrix of squared correlation coefficients for the variables in Eq. 2

	S_8^E(HOMO-1)*	F_{30}(LUMO+1)*	S_{21}^N(LUMO+2)*	μ_{16}^*
F_{30}(LUMO+1)*	0.07	1.00		
S_{21}^N(LUMO+2)*	0.06	0.04	1.00	
μ_{16}^*	0.03	0.15	0.11	1.00
S_{16}^N(LUMO+2)*	0.00	0.07	0.01	0.01

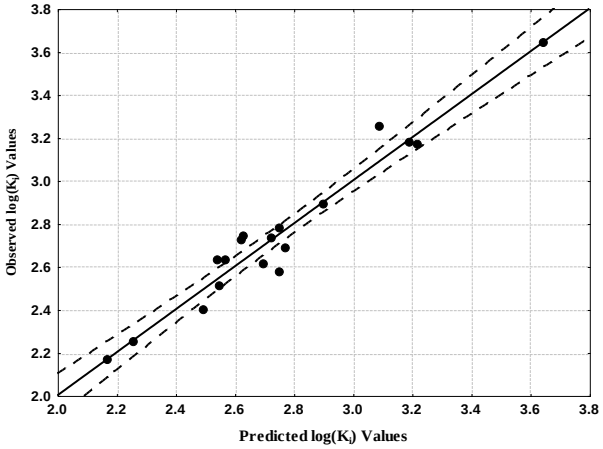

Figure 4: Plot of predicted vs. observed log(K_i) values (Eq. 2). Dashed lines denote the 95% confidence interval

The associated statistical parameters of Eq. 2 indicate that this equation is statistically significant and that the variation of the numerical values of a group of five local atomic reactivity indices of atoms of the common skeleton explains about 93% of the variation of the 5-HT_{2A} receptor affinity. Figure 4, spanning about 1.5 orders of magnitude, shows that there is a good correlation of observed *versus* calculated values.

Results for 5-HT_6 receptor binding affinity

The best equation obtained was:

$$\log(K_i)=5.69-0.95S_2^E(\text{HOMO-1})^*+0.25\mu_{22}^*-0.48F_{19}(\text{HOMO-2})^*+0.91\mu_{29}^* \quad (3)$$

with n=18, R=0.96, R^2=0.92, adj-R^2=0.90, F(4,13)=38.12 (p<0.000001) and SD=0.11. No outliers were detected and no residuals fall outside the ±2σ limits. Here, S_2^E(HOMO-1)* is the electrophilic superdelocalizability of the second highest local MO of atom 2, μ_{22}^* is the local electronic chemical potential of atom 22, F_{19}(HOMO-2)* is the Fukui index of the third highest local MO of atom 19 and μ_{29}^* is the local electronic chemical potential of atom 29.Tables 6 and 7 show the beta coefficients, the results of the t-test for significance of coefficients and the matrix of squared correlation coefficients for the variables of Eq. 3. There are no significant internal correlations between independent variables (Table 7), but we may observe that variables μ_{29} and F_{19}(HOMO-2)* has a relatively high correlation,

despite the fact that they belong to atoms that are not connected by aromatic systems. Figure 5 displays the plot of observed *vs.* calculated log(K_i).

Table 6: Beta coefficients and t-test for significance of coefficients in Eq. 3

	Beta	t(13)	p-level
S_2^E(HOMO-1)*	-0.97	-10.60	<0.000000
μ_{22}^*	0.28	3.33	0.005
F_{19}(HOMO-2)*	-0.64	-5.78	0.00006
μ_{29}^*	0.52	4.51	0.0006

Table 7: Matrix of squared correlation coefficients for the variables in Eq. 3

	S_2^E(HOMO-1)*	μ_{22}^*	F_{19}(HOMO-2)*
μ_{22}^*	0.03	1.00	
F_{19}(HOMO-2)*	0.06	0.05	1.00
μ_{29}^*	0.03	0.11	0.38

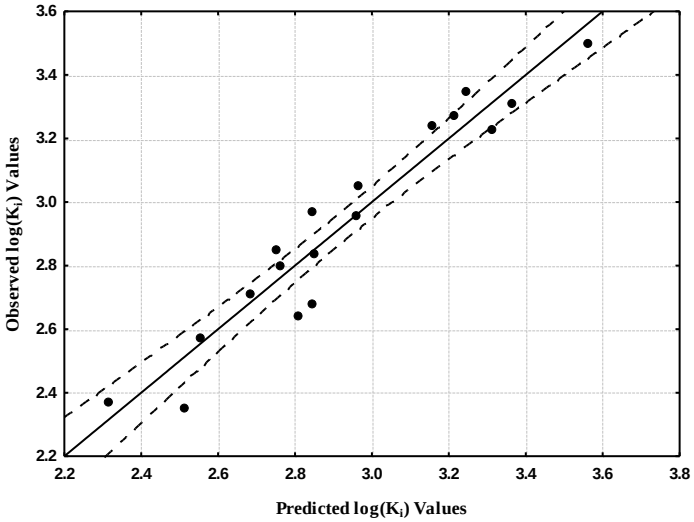

Figure 5: Plot of predicted vs. observed log(K_i) values (Eq. 3). Dashed lines denote the 95% confidence interval

The associated statistical parameters of Eq. 3 indicate that this equation is statistically significant and that the variation of the numerical values of a group of four local atomic reactivity indices of atoms of the common skeleton explains about 90% of the variation of the 5-HT_6 receptor affinity. Figure 5, spanning about 1.3 orders of magnitude, shows that there is a good correlation of observed *versus* calculated values.

Results for 5-HT_7serotonin receptor binding affinity

The best equation obtained was:

$$\log(K_i) = 4.79 + 3.83F_{28}(\text{LUMO}+1)^* + 1.14S_8^E(\text{HOMO})^* + 0.01S_{29}^N(\text{LUMO})^* + \\ +0.53S_{22}^N(\text{LUMO})^* - 3.15F_{18}(\text{HOMO}-2)^* - 0.26F_{19}(\text{HOMO}-2)^* \quad (4)$$

with n=18, R=0.98, R^2=0.96, adj-R^2=0.94, F(6,11)=46.30 (p<0.000001) and SD=0.20. No outliers were detected and no residuals fall outside the ±2σ limits. Here, F_{28}(LUMO+1)* is the Fukui index of the second lowest local MO of atom 28, S_8^E(HOMO)* is the electrophilic superdelocalizability of the highest occupied local MO of atom 8, S_{29}^N(LUMO)* is the nucleophilic superdelocalizability of the lowest empty local MO of atom 29, S_{22}^N(LUMO)* is the nucleophilic superdelocalizability of the lowest empty local MO of atom 22, F_{18}(HOMO-2)* is the Fukui index

of the third highest occupied local MO of atom 18 and F_{19}(HOMO-2)* is the Fukui index of the third highest occupied local MO of atom 18. Tables 8 and 9 show the beta coefficients, the results of the t-test for significance of coefficients and the matrix of squared correlation coefficients for the variables of Eq. 4. There are no significant internal correlations between independent variables (Table 9). Figure 6 displays the plot of observed *vs.* calculated $\log(K_i)$.

Table 8: Beta coefficients and t-test for significance of coefficients in Eq. 4

	Beta	t(11)	p-level
F_{28}(LUMO+1)*	0.87	12.14	<0.000000
S_8^E(HOMO)*	0.47	7.46	0.00001
S_{29}^N(LUMO)*	0.38	5.86	0.0001
S_{22}^N(LUMO)*	0.28	4.64	0.0007
F_{18}(HOMO-2)*	-0.20	-3.15	0.009
F_{19}(HOMO-2)*	-0.15	-2.25	0.05

Table 9: Matrix of squared correlation coefficients for the variables in Eq. 4

	F_{28}(LUMO+1)*	S_8^E(HOMO)*	S_{29}^N(LUMO)*	S_{22}^N(LUMO)*	F_{18}(HOMO-2)*
S_8^E(HOMO)*	0.03	1.00			
S_{29}^N(LUMO)*	0.12	0.02	1.00		
S_{22}^N(LUMO)*	0.00	0.01	0.02	1.00	
F_{18}(HOMO-2)*	0.11	0.01	0.04	0.02	1.00
F_{19}(HOMO-2)*	0.19	0.06	0.04	0.00	0.01

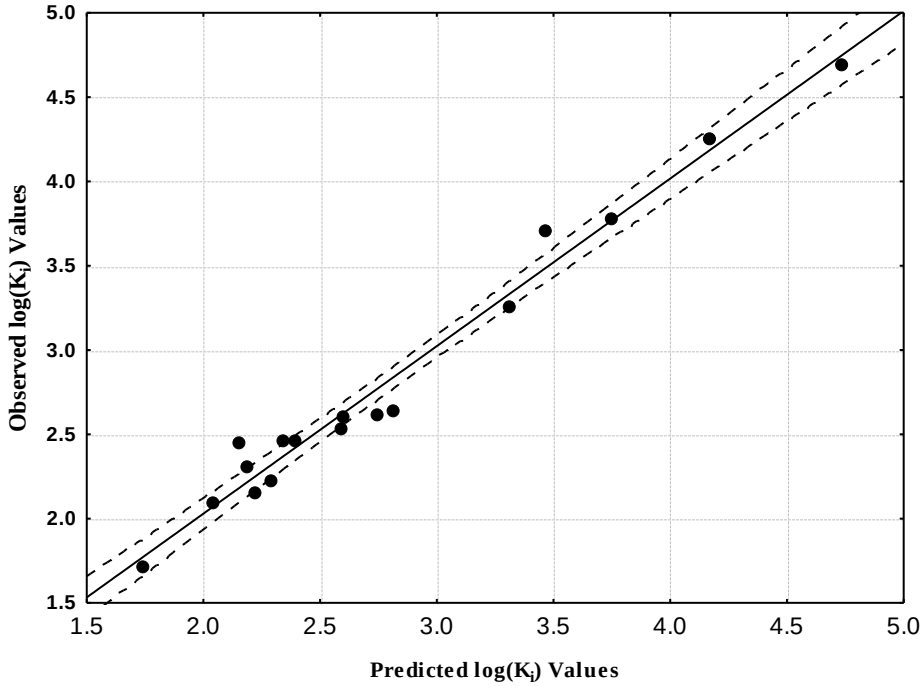

Figure 6: Plot of predicted vs. observed log(K_i) values (Eq. 4). Dashed lines denote the 95% confidence interval

The associated statistical parameters of Eq. 4 indicate that this equation is statistically significant and that the variation of the numerical values of a group of six local atomic reactivity indices of atoms constituting the common skeleton explains about 94% of the variation of the 5-HT_7 receptor affinity.Figure 6, spanning about 3 orders of magnitude, shows that there is a good correlation of observed *versus* calculated values and that almost all points are inside the 95% confidence interval.

Results for D_2dopamine receptor binding affinity

The best equation obtained was:

$$\log(K_i) = 8.17 + 4.30S_{19}^{N}(\mathrm{LUMO}+1)^* - 2.09S_{7}^{E}(\mathrm{HOMO}-1)^* - \\ -1.12S_{20}^{N}(\mathrm{LUMO}+2)^* - 0.08S_{25}^{N}(\mathrm{LUMO}+2)^* + 0.64S_{27}^{E} \quad (5)$$

with n=18, R=0.99, R^2=0.97, adj-R^2=0.96, F(5,12)=92.47 (p<0.000001) and SD=0.06. No outliers were detected and no residuals fall outside the ±2σ limits. Here, S_{19}^{N}(LUMO+1)* is the nucleophilic superdelocalizability of the second lowest empty local MO of atom 19, S_7^{E}(HOMO-1)* is the electrophilic superdelocalizability of the second highest occupied local MO of atom 7, S_{20}^{N}(LUMO+2)* is the nucleophilic superdelocalizability of the third lowest empty local MO of atom 20, S_{25}^{N}(LUMO+2)* is the nucleophilic superdelocalizability of the third lowest empty local MO of atom 25 and S_{27}^{E} is the total atomic nucleophilic superdelocalizability of atom 27.Tables 10 and 11 show the beta coefficients, the results of the t-test for significance of coefficients and the matrix of squared correlation coefficients for the variables of Eq. 5. There are no significant internal correlations between independent variables (Table 11). Figure 7 displays the plot of observed *vs.* calculated log(K_i).

Table 10: Beta coefficients and t-test for significance of coefficients in Eq. 5

	Beta	**t(12)**	**p-level**
S_{19}^{N}(LUMO+1)*	0.71	15.12	<0.000000
S_7^{E}(HOMO-1)*	-0.91	-15.76	<0.000000
S_{20}^{N}(LUMO+2)*	-0.53	-9.93	<0.000000
S_{25}^{N}(LUMO+2)*	-0.42	-7.83	0.000005
S_{27}^{E}	0.30	5.28	0.0002

Table 11: Matrix of squared correlation coefficients for the variables in Eq. 5

	S_{19}^{N}(LUMO+1)*	**S_7^{E}(HOMO-1)***	**S_{20}^{N}(LUMO+2)***	**S_{25}^{N}(LUMO+2)***
S_7^{E}(HOMO-1)*	0.03	1.00		
S_{20}^{N}(LUMO+2)*	0.00	0.19	1.00	
S_{25}^{N}(LUMO+2)*	0.00	0.03	0.08	1.00
S_{27}^{E}	0.01	0.20	0.04	0.21

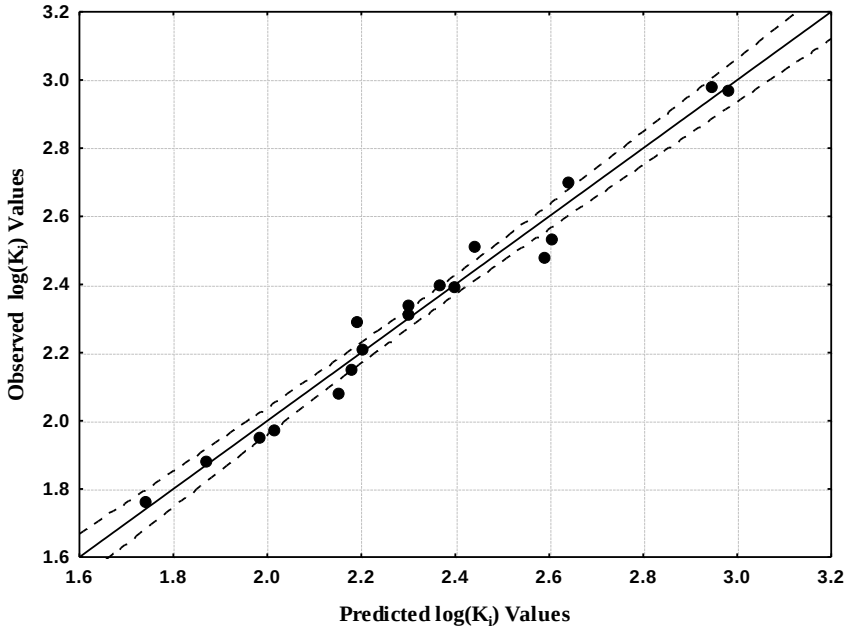

Figure 7: Plot of predicted vs. observed log(K_i) values (Eq. 5). Dashed lines denote the 95% confidence interval

The associated statistical parameters of Eq. 5 indicate that this equation is statistically significant and that the variation of the numerical values of a group of five local atomic reactivity indices of atoms constituting the common skeleton explains about 96% of the variation of the D_2 dopamine receptor affinity. Figure 7, spanning about 1.3 orders of magnitude, shows that there is a good correlation of observed *versus* calculated.

Local Molecular Orbitals

Tables 12 to 14 show the local molecular orbital structure of atoms appearing in equations 1-5.

Table 12: Local molecular orbitals of atoms 2, 7, 8, 14 and 16

Mol.	Atom 2	Atom 7	Atom 8	Atom 14	Atom 16
1 (124)	119π120π123π-	119π122σ123π-	119π122σ123π-	117σ119σ123σ-	115σ116σ122σ-
	125π126π129π	125π126π129π	125π126π129π	129σ134σ135σ	145σ148σ149σ
2(128)	123π125σ127π-	122σ123π127π-	118σ121σ127π	121σ122σ127σ-	116σ117σ118σ-
	129π130π132σ	129π134π135π	-129π134π135π	141σ142σ143σ	140σ146σ148σ
3(128)	123π124π127π-	121π123π127π-	121π123π127π-	121σ123σ127σ-	118σ119σ126σ-
	129π130π133π	129π130π133π	129π130π133π	133σ139σ140σ	141σ145σ146σ
4(128)	123π125σ127π-	122σ123π127π-	118σ120σ127π	120σ122σ127σ-	117σ118σ126σ-
	129π130π132σ	129π134σ135π	-129π134π135π	138σ139σ141σ	138σ140σ144σ
5(136)	131π133σ136π-	130σ131π136π-	126σ129σ136π	129σ130σ136σ-	124σ125σ126σ-
	137π138π141σ	137π142σ144π	-137π142σ144π	146σ150σ152σ	146σ153σ158σ
6(136)	131π132π135π-	129π131π135π-	129π131π135π-	129σ131σ135σ-	124σ125σ127σ-
	137π138π142π	137π138π142π	137π138π142π	143σ149σ155σ	145σ150σ152σσ
7(136)	132π133σ136π-	130σ132π136π-	127σ129σ136π	129σ130σ136σ-	125σ126σ127σ-
	137π138π140σ	137π142σ143π	-137π142σ143π	145σ148σ154σ	145σ148σ151σ
8(136)	132π134π135π-	131π134π135π-	129π134π135π-	131σ134σ135σ-	126σ127σ128σ-
	137π138π141π	137π138π141π	137π138π141π	146σ148σ149σ	153σ154σ156σ
9(115)	110π111π114π-	111π113σ114π-	107π113σ114π-	110σ111σ114σ-	106σ107σ113σ-
	116π117π120π	116π117π120π	116π120π122σ	120σ126σ130σ	123σ124σ126σ
10(119)	114π115π118π-	113σ115π118π-	110π111π118π-	114σ115σ118σ-	108σ109σ111σ-
	120π121π124π	120π121π124π	120π124π134σ	124σ130σ135σ	128σ130σ131σ
11(119)	114π115π118π-	115π117π118π-	110π117π118π-	114σ115σ118σ-	109σ110σ117σ-
	120π121π124π	120π121π124π	120π124π127σ	124σ129σ132σ	127σ128σ135σ
12(119)	114π116π118π-	113σ116π118π-	108π110π118π-	114σ116σ118σ-	109σ110σ117σ-
	120π121π124π	120π121π124π	120π124π127σ	124σ135σ137σ	128σ130σ131σ
13(127)	122π123π127π-	121σ123π127π-	117π118π127π-	122σ123σ127σ-	117σ118σ125σ-
	128π130π133π	128π130π133π	128π133π135σ	133σ137σ141σ	135σ138σ140σ
14(127)	122σ123π126π-	121σ123π126π-	116π118π126π-	122σ123σ126σ-	116σ118σ125σ-
	128π129π133π	128π129π133π	128π133π136σ	133σ143σ146σ	137σ139σ140σ
15(128)	123σ125π127π-	122σ125π127π-	117σ119π127π-	123σ125σ127σ-	116σ117σ119σ-
	129π130π134π	129π130π134π	129π134π135σ	134σ135σ138σ	135σ139σ142σ
16(127)	123σ124π126π-	122124π126π-	117σ119π126π-	123σ124σ126σ-	118σ119σ127σ-
	128π130π132π	128π130π132π	128π132π133π	134σ138σ141σ	135σ136σ142σ
17(127)	123π124π126π-	121σ124π126π-	118σ119π126π-	123σ124σ126σ-	118σ119σ125σ-
	128π130π132π	128π130π132π	128π132π134σ	132σ139σ142σ	135σ136σ138σ
18(127)	123π124π126π-	122σ124π126π-	117σ119π126π-	123σ124σ126σ-	118σ119σ125σ-
	128π129π132π	128π129π132π	128π132π135σ	132σ140σ143σ	135σ138σ139σ

Table 13: Local molecular orbitals of atoms 18, 19, 20, 21 and 22

Mol.	Atom 18	Atom 19	Atom 20	Atom 21	Atom 22
1 (124)	115σ122σ124σ-	122σ123σ124σ-	115σ122σ124σ-	118σ122σ124σ-	118σ122σ124σ-
	137σ138σ139σ	140σ141σ146σ	136σ138σ142σ	134σ135σ137σ	138σ142σ143σ
2(128)	117σ126σ128σ-	124σ126σ128σ-	117σ126σ128σ-	120σ126σ128σ-	120σ126σ128σ-
	139σ142σ144σ	149σ150σ152σ	144σ149σ150σ	144σ146σ148σ	143σ144σ149σ
3(128)	117σ118σ126σ-	117σ118σ126σ-	118σ122σ126σ-	122σ126σ128σ-	122σ126σ128σ-
	139σ140σ142σ	142σ148σ149σ	141σ142σ144σ	131σ132σ140σ	141σ143σ145σ
4(128)	116σ117σ126σ-	121σ126σ128σ-	121σ126σ128σ-	121σ126σ128σ-	116σ121σ126σ-
	140σ141σ143σ	141σ151σ152σ	141σ144σ145σ	140σ144σ149σ	141σ144σ145σ
5(136)	123σ125σ134σ-	128σ134σ135σ-	125σ134σ135σ-	122σ128σ135σ-	128σ134σ135σ-
	149σ150σ151σ	148σ150σ158σ	150σ152σ157σ	157σ158σ159σ	140σ151σ152σ
6(136)	124σ125σ134σ-	130σ134σ136σ-	130σ134σ136σ-	130σ134σ136σ-	123σ130σ134σ-
	143σ149σ150σ	149σ155σ157σ	150σ152σ153σ	149σ151σ154σ	150σ152σ153σ
7(136)	126σ127σ134σ-	128σ134σ135σ-	128σ134σ135σ-	128σ134σ135σ-	128σ134σ135σ-
	145σ147σ148σ	147σ153σ156σ	148σ151σ153σ	149σ153σ156σ	148σ149σ153σ
8(136)	126σ127σ135σ-	134σ135σ136σ-	134σ135σ136σ-	127σ130σ136σ-	134σ135σ136σ-
	144σ148σ149σ	150σ153σ154σ	149σ150σ152σ	149σ150σ152σ	148σ149σ150σ
9(115)	105σ106σ113σ-	113σ114σ115σ-	108σ113σ115σ-	108σ113σ115σ-	108σ113σ115σ-
	123σ125σ126σ	128σ131σ134σ	126σ128σ132σ	118σ119σ123σ	126σ127σ128σ
10(119)	109σ117σ119σ-	116σ117σ119σ-	112σ117σ119σ-	112σ117σ119σ-	109σ117σ119σ-
	129σ131σ132σ	133σ138σ142σ	138σ139σ140σ	123σ131σ133σ	131σ137σ138σ
11(119)	109σ110σ117σ-	117σ118σ119σ-	112σ117σ119σ-	112σ117σ119σ-	112σ117σ119σ-
	127σ128σ129σ	129σ135σ139σ	129σ132σ133σ	127σ134σ137σ	129σ131σ132σ
12(119)	108σ109σ117σ-	117σ118σ119σ-	112σ117σ119σ-	112σ117σ119σ-	109σ112σ117σ-
	127σ128σ129σ	139σ140σ142σ	129σ131σ132σ	128σ132σ134σ	129σ131σ132σ
13(127)	116σ117σ125σ-	117σ125σ126σ-	117σ125σ126σ-	120σ125σ126σ-	120σ125σ126σ-
	135σ137σ139σ	137σ143σ145σ	138σ140σ143σ	138σ145σ146σ	135σ143σ146σ
14(127)	115σ116σ125σ-	116σ125σ127σ-	120σ125σ127σ-	120σ125σ127σ-	116σ120σ125σ-
	136σ137σ138σ	138σ147σ148σ	138σ140σ141σ	137σ141σ143σ	138σ140σ141σ
15(128)	117σ126σ128σ-	121σ126σ128σ-	117σ126σ128σ-	121σ126σ128σ-	121σ126σ128σ-
	135σ138σ139σ	147σ148σ150σ	141σ142σ146σ	139σ140σ141σ	141σ144σ145σ
16(127)	118σ125σ127σ-	118σ125σ127σ-	117σ125σ127σ-	121σ125σ127σ-	120σ121σ127σ-
	134σ136σ138σ	143σ144σ145σ	135σ140σ143σ	136σ143σ144σ	136σ143σ144σ
17(127)	117σ118σ125σ-	120σ125σ127σ-	120σ125σ127σ-	120σ125σ127σ-	120σ125σ127σ-
	134σ135σ137σ	144σ149σ150σ	136σ139σ140σ	135σ139σ142σ	136σ137σ139σ
18(127)	118σ125σ127σ-	120σ125σ127σ-	120σ125σ127σ-	120σ125σ127σ-	117σ125σ127σ-
	136σ137σ140σ	147σ152σ157σ	137σ141σ142σ	130σ136σ137σ	136σ137σ142σ

Table 14: Local molecular orbitals of atoms 25, 26, 27, 28, 29 and 30

Mol.	Atom 25	Atom 26	Atom 27	Atom 28	Atom 29	Atom 30
1 (124)	118σ122π124π-	122π123σ124π-	121π122π124π-	111σ118π121π-	121π122π124π-	122π123σ124π-
	127π128π134σ	127π128π134σ	127π128π136σ	127π128π136σ	127π128π136σ	127π128π136σ
2(128)	120σ126π128σ-	124π126π128σ-	124π126π128σ-	119σ120π124π-	120π124π126π-	120π126π128σ-
	131π133π136σ	131π133π136σ	131π133π136σ	131π133π136σ	131π133π144σ	131π133π136σ
3(128)	122π125π128π-	122π125π128π-	122π125π128π-	122π125π128π-	122π125π128π-	122π125π128π-

	131π132π134σ	131π132π134σ	131π132π146σ	131π132π134σ	131π132π134σ	131π132π134σ
4(128)	121σ124π128π- 131π133π140σ	121σ124π128π- 131π133π136σ	121σ124π128π- 131π133π136σ	121π124π128π- 131π133π136σ	121π124π128π- 131π133π136σ	121π126σ128π- 131π133π136σ
5(136)	128σ134σ135π- 139π140π143σ	132π134σ135π- 139π140π143σ	132π134σ135π- 139π140π143σ	128π132π135π- 139π140π143σ	128π132π135π- 139π140π143σ	132π134σ135π- 139π140π143σ
6(136)	130σ134σ136π- 139π140π141σ	133π134σ136π- 139π140π141σ	133π134σ136π- 139π140π154σ	133π134σ136π- 139π140π141σ	130π133π136π- 139π140π141σ	133π134σ136π- 139π140π141σ
7(136)	128σ134σ135π- 139π141π149σ	131π134σ135π- 139π141π149σ	131π134σ135π- 139π141π149σ	128π131π135π- 139π141π156σ	128π131π135π- 139π141π149σ	131π134σ135π- 139π141π149σ
8(136)	123π130π136π- 139π140π149σ	133π135σ136π- 139π140π149σ	133π135σ136π- 139π140π149σ	130π133π136π- 139π140π152σ	130π133π136π- 139π140π155σ	130π135σ136π- 139π140π158σ
9(115)	108σ113σ115π- 118π119π123σ	112π113σ115π- 118π119π123σ	108σ112π115π- 118π119π123σ	106σ108π112π- 118π119π123σ	108π112π115π- 118π119π136σ	108π113σ115π- 118π119π124σ
10(119)	112σ117π119σ- 122π123π125σ	116π117π119σ- 122π123π125σ	116π117π119σ- 122π123π125σ	111σ112π116π- 122π123π125σ	112π116π117π- 122π123π131σ	112π117π119σ- 122π123π125σ
11(119)	112σ117σ119π- 122π123π125σ	112σ116π119π- 122π123π125σ	116π117σ119π- 122π123π137σ	112π116π119π- 122π123π125σ	112π116π119π- 122π123π125σ	112π117σ119π- 122π123π125σ
12(119)	112σ115π119π- 122π123π128σ	112σ115π119π- 122π123π125σ	112σ115π119π- 122π123π125σ	112π115π119π- 122π123π125σ	112π115π119π- 122π123π125σ	111π112π119π- 122π12π3125σ
13(127)	120σ125σ126π- 129π131π132σ	124π125σ126π- 129π131π132σ	124π125σ126π- 129π131π132σ	119σ120π124π- 129π131π132σ	120π124π126π- 129π131π132σ	124π125σ126π- 129π131π132σ
14(127)	120σ125σ127π- 130π131π132σ	120σ124π127π- 130π131π132σ	124π125σ127π- 130π131π143σ	120π124π127π- 130π131π132σ	120π124π127π- 130π131π132σ	124π125σ127π- 130π131π132σ
15(128)	124π126π128π- 131π132π137σ	124π126π128π- 131π132π133σ	124π126π128π- 131π132π133σ	124π126π128π- 131π132π133σ	124π126π128π- 131π132π133σ	124π126π128π- 131π132π133σ
16(127)	121σ125σ127σ- 129π131π136σ	120π121π125σ- 129π131π135σ	121σ125σ127σ- 129π131π136σ	120π121π125π- 129π131π136σ	120π121σ125π- 129π131π136σ	120π121π125σ- 129π131π143π
17(127)	120σ125σ127π- 129π131π137σ	122π125σ127π- 129π131π136σ	122π125σ127π- 129π131π136σ	120π122π127π- 129π131π145σ	120π122π127π- 129π131π143σ	122π125σ127π- 129π131π136σ
18(127)	120σ125π127π- 130π131π140σ	122σ125π127π- 130π131π136σ	122σ125π127π- 130π131π136σ	120σ121π122π- 130π131π136σ	122σ125π127π- 130π131π142σ	120σ125π127π- 130π131π136σ

Discussion

The Discussion section follows guidelines presented in previous articles [40, 41, 73].

Discussion of serotonin 5-HT_{1A} receptor binding affinity results

Table 2 shows that the importance of variables in Eq. 1 is S_8^E(HOMO-1)*> S_{14}^N(LUMO)*>> S_{21}^N = S_{21}^E(HOMO-1)*> F_{26}(LUMO+2)*. The analysis of Eq. 1 shows that a high serotonin 5-HT_{1A} receptor binding affinity is associated with small (negative) values for S_8^E(HOMO-1)*, large (positive) values for S_{14}^N(LUMO)*, small values for S_{21}^N, small (negative) values fo rS_{21}^E(HOMO-1)* and large values for F_{26}(LUMO+2)*. Atom 8 is a carbon atom in ring A (Fig. 2). The local $(HOMO)_8$* has a π nature in all molecules while $(HOMO-1)_8$* has a σ or π nature (Table 12). Fig. 8 shows the local (HOMO)8* of molecule 1.

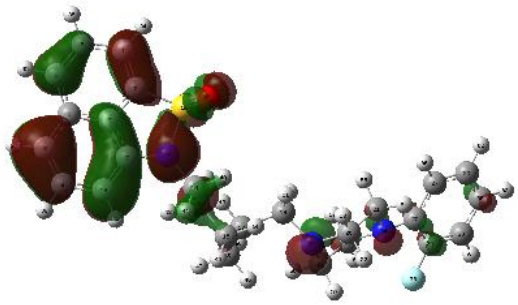

Figure 8: Local $(HOMO)_8$ of molecule 1 (see Fig. 2 for atom numbering)*

$LUMO_8$* coincides with the molecular LUMO in all molecules (Table 12). A small (negative) value of S_8^E(HOMO-1)* is obtained by lowering the MO energy, lowering the Fukui index of $(HOMO-1)_8$* or using both procedures simultaneously. In all cases the electron donating capacity of this MO is reduced. Now, if we accept that the same reasoning can be applied to $(HOMO)_8$* then we suggest that atom 8 is acting as an electron-acceptor and is engaged most probably in a π-π interaction, participating alone or together with one or more atoms of ring A. Atom 14 is a saturated carbon atom inside the chain linking rings C and D (Fig. 2). All local MOs have a σ nature (Table 12). A high serotonin5-HT_{1A} receptor affinity is associated with large (positive) values of S_{14}^N(LUMO)*. Figure 9 shows $(LUMO)_{14}^*$ of molecule 2.

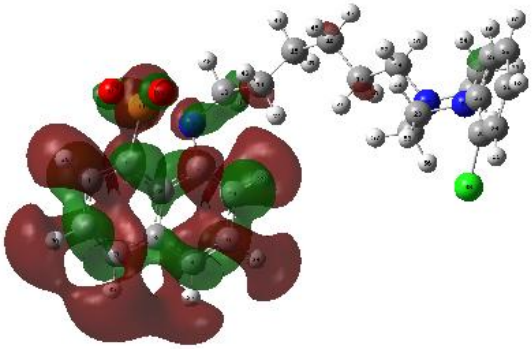

Figure 9: $(LUMO)_{14}^*$ of molecule 2 (see Fig. 2 for atom numbering)

These large values can be obtained by lowering the MO energy making $(LUMO)_{14}$* more reactive. For this reason we suggest that atom 14 is participating in a σ-π (with an aromatic system) or in an alkyl interaction (with aliphatic amino acid side-chains).Atom 21 is a saturated carbon atom in ring D (Fig. 2). All local MOs have a σ nature (Table 13). A high receptor affinity is associated with small values of S_{21}^N and small (negative) values of S_{21}^E(HOMO-1)*. Table 2 shows that both reactivity indices show similar beta values and t-test results. Regarding S_{21}^N, we know that the dominant term is S_{21}^N(LUMO)*. Therefore the process for obtaining small values will transform atom 21 in a very bad electron acceptor. On the other hand, small negative values for S_{21}^E(HOMO-1)* are obtained by shifting downwards (i.e., increasing the negative energy) of this local MO making this atom also a bad electron donor. The only hypothesis we can offer for these two facts (appearing for the first time) is that atom 21 is close to a 3D neutral area formed by atoms that should be also bad electron donors and bad electron acceptors. Atom 26 is a carbon atom in ring E (Fig. 2). Large values of F_{26}(LUMO+2)* are linked to high affinity. This immediately suggests that atom 26 is interacting with an electro-rich center probably through π-π interactions.All the suggestions are displayed in the partial 2D pharmacophore of Fig. 10.

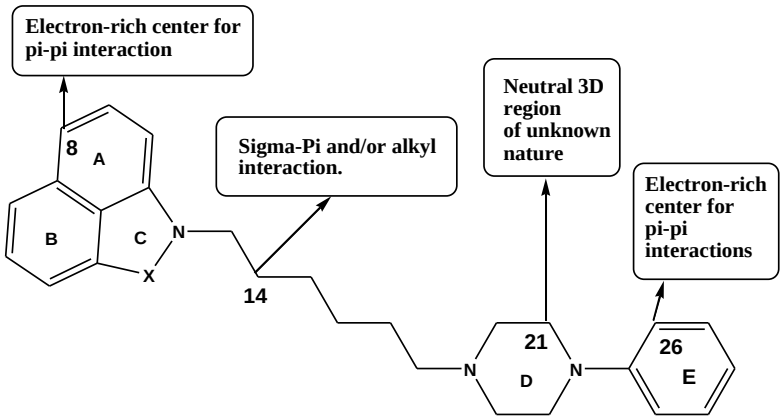

Figure 10: Partial 2D pharmacophore for serotonin5-HT$_{1A}$ receptor binding affinity

Discussion of serotonin 5-HT$_{2A}$ receptor binding affinity results

Table 4 shows that the importance of variables in Eq. 2 is F_{30}(LUMO+1)*>S_8^E(HOMO-1)*>S_{21}^N(LUMO+2)*>μ_{16}^*>>S_{16}^N(LUMO+2)*. Because of the t-test results S_{16}^N(LUMO+2)* will not be discussed. A high serotonin 5-HT$_{2A}$ receptor binding affinity is associated with small (negative) numerical values of S_8^E(HOMO-1)*, large numerical values of F_{30}(LUMO+1)* and S_{21}^N(LUMO+2)*, and with small (negative) values of μ_{16}^*. Atom 8 is a carbon atom in ring A (Fig. 2). Small (negative) numerical values of S_8^E(HOMO-1)* are associated with a high serotonin5-HT$_{2A}$ receptor affinity. With the same reasoning used for this atom in the case of serotonin 5-HT$_{2A}$ receptor we suggest that atom 8 is engaged most probably in a π-π interaction with an electron-rich center, participating alone or together with one or more atoms of ring A. Atom 30 is a carbon atom in ring E (Fig. 2). For a higher receptor affinity we need larger numerical values for F_{30}(LUMO+1)*. This suggests that atom 30 is interacting with an electron-rich center through at least its first two lowest empty local MOs. Table 14 shows that $(LUMO)_{30}^*$ and $(LUMO+1)_{30}^*$ have a π nature. Figure 11 shows the $(LUMO+1)_{30}^*$ of molecule 3.

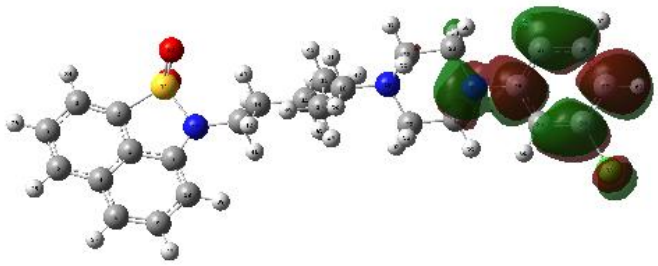

Figure 11: $(LUMO+1)_{30}^*$ of molecule 3 (see Fig. 2 for atom numbering)

Therefore the interaction is probably of the π-π kind but a π-σ interaction cannot be ruled out. Atom 21 is a saturated carbon atom in ring D (Fig. 2). All local MOs have a σ nature (Table 13). A high receptor affinity is associated with large numerical values for S_{21}^N(LUMO+2)*. These values are obtained by shifting downwards the MO energy, making this MO more reactive. Therefore, we suggest that this atom is interacting with an electron-rich center through σ-π and/or alkyl interactions. Atom 16 is a saturated carbon atom in the chain linking rings C and D (Fig. 2). Small (negative) values for μ_{16}^* are associated with high receptor affinity. Remembering that this local atomic reactivity index corresponds in this case to half of the $(HOMO)_{16}$*-$(LUMO)_{16}$* gap, a small negative value means that the $(HOMO)_{16}$* energy is shifting toward zero, making this atom a better electron donor. Figure 12 shows the $(HOMO)_{16}$* of molecule 4.

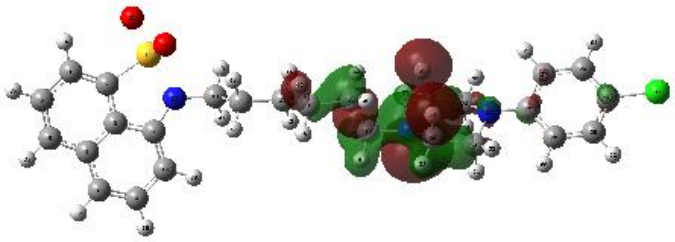

Figure 12: $(HOMO)_{16}$ of molecule 4 (see Fig. 2 for atom numbering)*

This suggests that atom 16 is interacting with an electron-deficient center (through alkyl, σ-π and/or σ-cation interactions). All the suggestions are displayed in the partial 2D pharmacophore of Fig. 13.

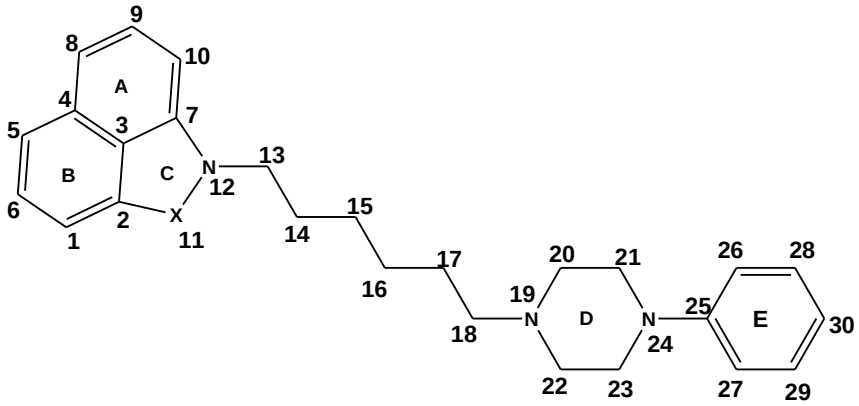

Figure 13: Partial 2D pharmacophore for serotonin 5-HT_{2A} receptor binding affinity

Discussion of serotonin 5-HT_6 receptor binding affinity results

Table 6 shows that the importance of variables in Eq. 3 is S_2^E(HOMO-1)*>>F_{19}(HOMO-2)*>μ_{29}^*>>μ_{22}^*. A high serotonin 5-HT_6 receptor binding affinity activity is associated with small (negative) numerical values for S_2^E(HOMO-1)*, large numerical values for F_{19}(HOMO-2)*, large (negative) values for μ_{29}^* and μ_{22}^*. Atom 2 is a carbon atom belonging to rings B and C (Fig. 2). Small (negative) numerical values for S_2^E(HOMO-1)* are associated with high affinity. Those small values make atom 2 a bad electron donor. If we accept the hypothesis that the same condition holds for S_2^E(HOMO)* and that this index is not appearing in Eq. 3 only because it is not statistically significant, then we suggest that atom 2 is interacting with en electron-rich center. The other way to get small values for S_2^E(HOMO-1)* and S_2^E(HOMO)* is by removing the localization of these specific local MOs on atom 21. Table 12 shows that $(LUMO)_2$*and$(LUMO+1)_2$* have a π nature. Figure 14 shows $(LUMO)_2$* of molecule 5.

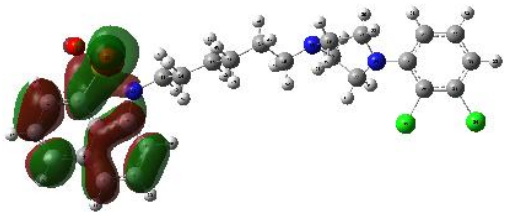

Figure 14: $(LUMO)_2$ of molecule 5 (see Fig. 2 for atom numbering)*

Therefore, the most probable interaction is a π-π one. Atom 19 is one of the nitrogen atoms of ring D (Fig. 2). All local MOs have not a π nature (Table 13). Large numerical values for F_{19}(HOMO-2)* are associated with high affinity. This suggests that atom19 is interacting with an electron-deficient center (note that $(LUMO)_{19}$* corresponds to a higher empty MO). This interaction seems to be an alkyl one. Atom 29 is a carbon atom of ring E (Fig. 2). A high affinity is associated with large (negative) numerical values for μ_{29}^*. These values are obtained by shifting

downwards the $(HOMO)_{29}$* energy, making this MO less reactive and $(LUMO)_{29}$* more reactive. For this reason we suggest that atom 29 is interacting with an electron-rich center. Table 14 shows that the two lowest empty local MOs have a π nature. Therefore the interaction can be of the π-π, π-σ and/or π-anion kinds. Atom 22 is a saturated carbon atom of ring D (Fig. 2). Large (negative) numerical values for μ_{22}^{*} are associated with high receptor affinity. Following a similar reasoning employed for atom 29, we suggest that atom 22 interacts with an electron-rich center. Table 13 shows that all local MOs have a σ nature. Figure 15 shows $(LUMO)_{22}$* of molecule 6.

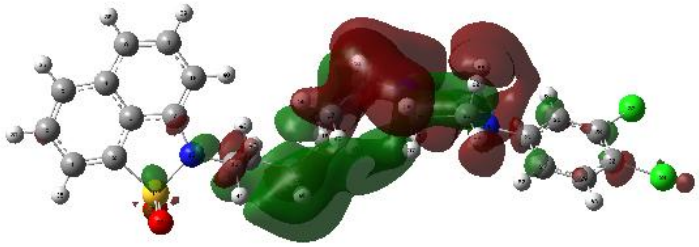

Figure 15: $(LUMO)_{22}$ of molecule 6 (see Fig. 2 for atom numbering)*

Therefore the interaction can be of the σ-anion, alkyl and/or σ-π kinds. All the suggestions are displayed in the partial 2D pharmacophore of Fig. 16.

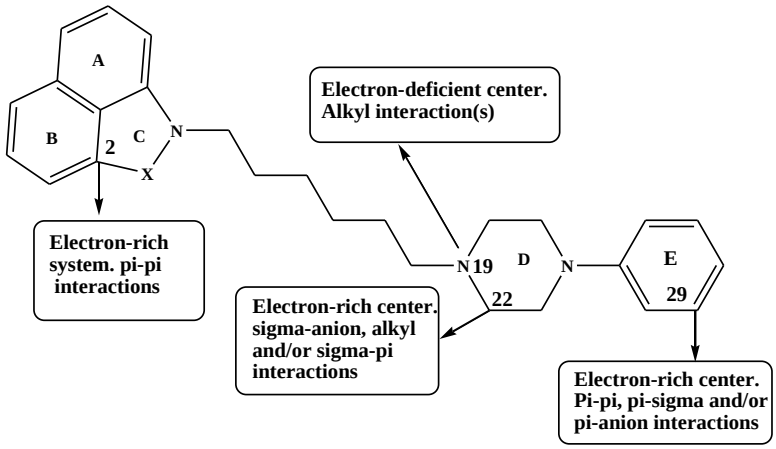

Figure 16: Partial 2D pharmacophore for serotonin5-HT_6 receptor binding affinity

Discussion of serotonin 5-HT_7 receptor binding affinity results

Table 8 shows that the importance of variables in Eq. 4 is F_{28}(LUMO+1)*>> S_8^{E}(HOMO)* >S_{29}^{N}(LUMO)*>S_{22}^{N}(LUMO)*>F_{18}(HOMO-2)*>F_{19}(HOMO-2)*. Because of the t-test results, F_{18}(HOMO-2)* and F_{19}(HOMO-2)* will not be discussed. A high serotonin 5-HT_7 receptor activity is associated with small numerical values for F_{28}(LUMO+1)*, large (negative) numerical values for S_8^{E}(HOMO)*, small numerical values for S_{29}^{N}(LUMO)* and small numerical values for S_{22}^{N}(LUMO)*.Atom 28 is a carbon atom in ring E (Fig. 2). Small numerical values for F_{28}(LUMO+1)* are associated with high 5-HT_7receptor affinity. These types of values are obtained by lowering the localization of $(LUMO+1)_{28}^{*}$. An ideal situation is when F_{28}(LUMO+1)*=0. If $(LUMO+1)_{28}^{*}$ follows the same trend atom 20 will behave as a bad electron acceptor. On the other hand, Table 14 shows that in all cases $(HOMO)_{28}^{*}$ has a π character. Figure 17 shows $(HOMO)_{28}^{*}$ of molecule 7.

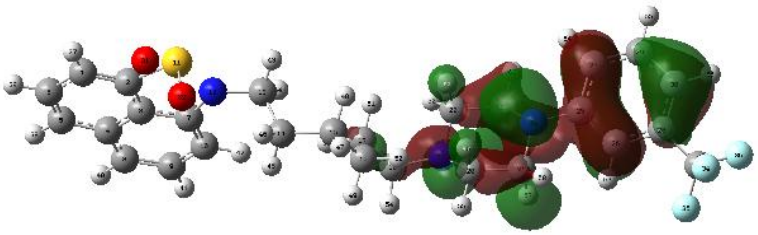

Figure 17: $(HOMO)_{28}^{*}$ of molecule 7 (see Fig. 2 for atom numbering)

On this basis we suggest that atom 28 is interacting with an electron-rich moiety through π-π, π-σ and /or alkyl interactions. Atom 8 is a carbon atom in ring A (Fig. 2). Large (negative) numerical values for S_8^E(HOMO)* are required for high receptor affinity. Table 12 shows that $(HOMO)_8$* has a π nature in all cases. Large negative values are obtained by shifting upwards the $(HOMO)_8$* energy (i.e., approaching it to zero) making this MO more reactive. Therefore it is suggested that this atom interacts with an electron-deficient center through π-π and/or π-cation interactions. Atom 29 is a carbon atom in ring E (Fig. 2). Small numerical values for S_{29}^N(LUMO)* are associated with high receptor affinity. These types of values are obtained by enlarging the MO energy making it less reactive. The ideal case is when S_{29}^N(LUMO)*→0. On the other hand, Table 14 shows that $(HOMO)_{29}$* has a π nature in all molecules. Figure 18 shows the $(HOMO)_{29}$* of molecule 8.

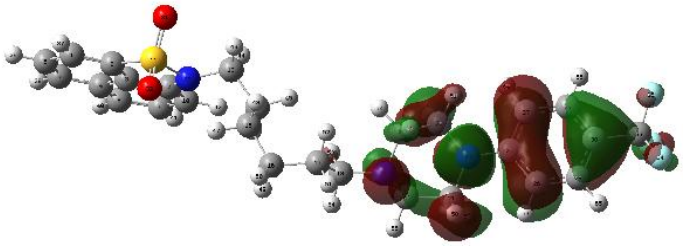

Figure 18: $(HOMO)_{29}$ of molecule 8 (see Fig. 2 for atom numbering)*

We suggest that atom 29 is interacting with an electron-deficient center through π-cation and/or π-π interactions. Atom 22 is a saturated carbon atom in ring D (Fig. 2). All local MOs have not a π nature (Table 13). A high receptor affinity is associated with small numerical values for S_{22}^N(LUMO)*. Table 13 shows that $(LUMO)_{22}^*$ does not coincide with the molecular LUMO and that it corresponds to a very high empty molecular MO. Therefore atom 22 behaves as a very bad electron donor. Considering that $(HOMO)_{22}^*$ coincides with the molecular HOMO, HOMO-1 or HOMO-2 it is possible to suggest that this atom is interacting with an electron deficient center through σ-cation, σ-π or alkyl interactions. All the suggestions are displayed in the partial 2D pharmacophore of Fig. 19.

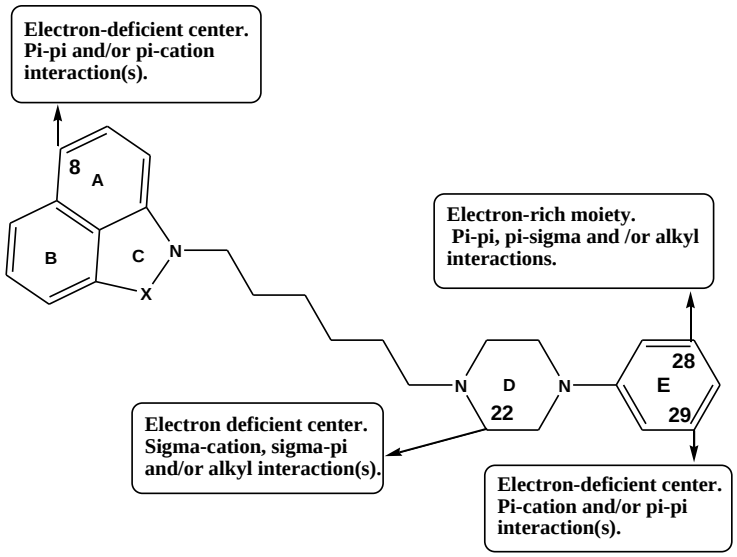

Figure 19: Partial 2D pharmacophore for serotonin 5-HT_7 receptor affinity

Discussion of the dopamineD_2 receptor binding affinity results

Table 10 shows that the importance of variables in Eq. 5 is S_7^E(HOMO-1)*>>S_{19}^N(LUMO+1)*> S_{20}^N(LUMO+2)*>S_{25}^N(LUMO+2)*>S_{27}^E. Because of the t-test result S_{27}^E will not be discussed. A high dopamine D_2 receptor affinity is associated with small numerical (negative) values for S_7^E(HOMO-1)*, small numerical values for S_{19}^N(LUMO+1)*, large numerical values for S_{20}^N(LUMO+2)* and S_{25}^N(LUMO+2)*. Atom 7 is a carbon atom in

rings A and C (Fig. 2). Small numerical (negative) values for S_7^E(HOMO-1)* are associated with high dopamine D_2 receptor affinity. Small values are obtained by decreasing the location of this MO on atom 7 or by making its energy more negative. If S_7^E(HOMO)* follows the same trend, then atom 7 is behaving as a bad electron donor. On the other hand $(LUMO)_7$* has a π nature in all molecules (Table 12) and coincides with the molecular LUMO. Figure 20 shows the $(LUMO)_7$* of molecule 9.

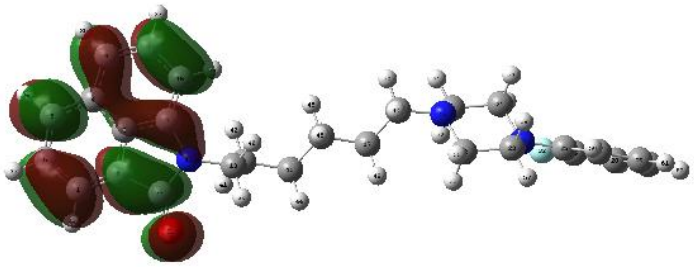

Figure 20: $(LUMO)_7$ of molecule 9 (see Fig. 2 for atom numbering)*

We suggest then that atom 7 is interacting with an electron-rich center through π-π or π-anion interactions. Atom 19 is a nitrogen atom in ring D (Fig. 2). All local MOs have not a π nature. A high receptor affinity is associated with small numerical values for S_{19}^N(LUMO+1)*. These values transform atom 19 in a bad electron acceptor. This is consistent with the fact that this MO is energetically very far from the molecular LUMO (see Table 13). This Table also show that $(HOMO)_{19}^*$ coincides with the molecular HOMO, HOMO-1 or HOMO-2. For these reasons we suggest that atom 19 is interacting with an electron deficient center through σ-cation, σ-π and/or alkyl interactions. Atom 20 is a saturated carbon atom in ring D (Fig. 2). All local MOs have not a π nature. Large numerical values for S_{20}^N(LUMO+2)* are needed for high receptor affinity. These values are obtained by shifting downwards the MO energy (i.e., toward zero) making $(LUMO+2)_{20}^*$ more reactive. This also makes $(LUMO+1)_{20}^*$ and $(LUMO)_{20}^*$ more reactive. Table 13 shows that $(LUMO)_{20}^*$ is very far from the molecular LUMO. This is an interesting fact to explore by experiment or by theory, trying to determine if there is a way to lower $(LUMO)_{20}^*$. If our results are correct this could open an interesting way to explore the real role that ring D plays in determining receptor affinity. We tentatively suggest that atom 20 is facing an electron-rich center. The interactions can be of the σ-anion and/or σ-π kinds. Atom 25 is a carbon atom in ring E (Fig. 2). Large numerical values for S_{25}^N(LUMO+2)* are needed for a high D_2 dopamine receptor affinity. Large values for this index are obtained by shifting toward zero the energy of $(LUMO+2)_{25}^*$, making it more reactive. This, in turn, will also make $(LUMO+1)_{25}^*$ and $(LUMO)_{25}^*$ more reactive. Table 14 shows that $(LUMO+1)_{25}^*$ and $(LUMO)_{25}^*$ have a π nature while $(LUMO+2)_{25}^*$ is a σ MO in all cases. Figure 21 shows the $(LUMO+2)_{25}^*$ of molecule 10.

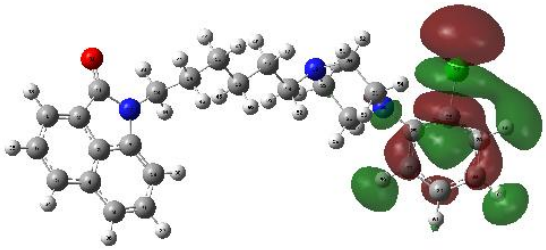

Figure 21: $(LUMO+2)_{25}^*$ of molecule 10 (see Fig. 2 for atom numbering)

It would be interesting to explore the effects on receptor affinity when the three lowest empty local MOs of this atom have of a π nature. It is suggested that atom 25 is interacting with an electron-rich moiety through π-π, π-anion and/or π-σ interactions. All the suggestions are displayed in the partial 2D pharmacophore of Fig. 22.

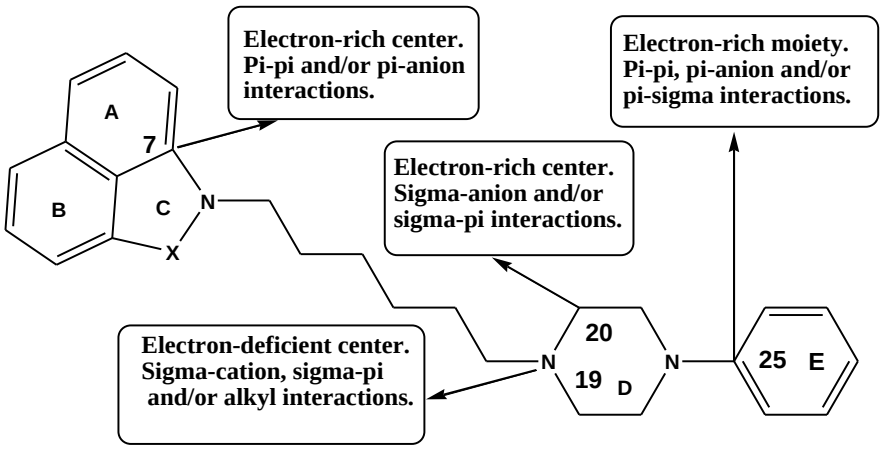

Figure 22: Partial 2D pharmacophore for dopamine D_2 receptor affinity

In summary, we have obtained statistically significant relationships between the electronic structure and the receptor binding affinity one dopaminergic (D_2) and four serotonergic (5-HT_{1A}, 5-HT_{2A}, 5-HT_6, 5-HT_7) receptors for a series of fananserin derivatives. All the QSAR results show again that sigma molecular orbitals in rings and/or linkers are playing a role in the molecule-receptor interaction.

References

[1]. Schmidt, C.; Skandali, N.; Gleesborg, C.; Kvamme, T. L.; Schmidt, H.; Frisch, K.; Møller, A.; Voon, V. The role of dopaminergic and serotonergic transmission in the processing of primary and monetary reward. Neuropsychopharmacology 2020, 1-8.

[2]. Lak, A.; Okun, M.; Moss, M. M.; Gurnani, H.; Farrell, K.; Wells, M. J.; Reddy, C. B.; Kepecs, A.; Harris, K. D.; Carandini, M. Dopaminergic and prefrontal basis of learning from sensory confidence and reward value. Neuron 2020, 105, 700-711. e6.

[3]. Ben-Jonathan, N. Dopamine: endocrine and oncogenic functions. CRC Press: Boca Raton, FL, 2020.

[4]. Vidal, P. M.; Pacheco, R. Targeting the dopaminergic system in autoimmunity. Journal of Neuroimmune Pharmacology 2019, 1-17.

[5]. Kalisch, R.; Gerlicher, A. M.; Duvarci, S. A dopaminergic basis for fear extinction. Trends in cognitive sciences 2019, 23, 274-277.

[6]. Fiory, F.; Perruolo, G.; Cimmino, I.; Cabaro, S.; Pignalosa, F. C.; Miele, C.; Beguinot, F.; Formisano, P. The relevance of insulin action in the dopaminergic system. Frontiers in neuroscience 2019, 13, 868.

[7]. Tricklebank, M. D.; Daly, E. The Serotonin System: History, Neuropharmacology, and Pathology. Academic Press - Elsevier: London, 2019.

[8]. Zhang, C.; Li, Q.; Meng, L.; Ren, Y. Design of novel dopamine D2 and serotonin 5-HT2A receptors dual antagonists toward schizophrenia: An integrated study with QSAR, molecular docking, virtual screening and molecular dynamics simulations. Journal of Biomolecular Structure and Dynamics 2020, 38, 860-885.

[9]. Wróbel, M. Z.; Chodkowski, A.; Marciniak, M.; Dawidowski, M.; Maksymiuk, A.; Siwek, A.; Nowak, G.; Turło, J. Synthesis of new 4-butyl-arylpiperazine-3-(1H-indol-3-yl) pyrrolidine-2, 5-dione derivatives and evaluation for their 5-HT1A and D2 receptor affinity and serotonin transporter inhibition. Bioorganic Chemistry 2020, 97, 103662.

[10]. Jin, J.; Zhang, K.; Dou, F.; Hao, C.; Zhang, Y.; Cao, X.; Gao, L.; Xiong, J.; Liu, X.; Liu, B.-F. Isoquinolinone derivatives as potent CNS multi-receptor D2/5-HT1A/5-HT2A/5-HT6/5-HT7 agents: Synthesis and pharmacological evaluation. European Journal of Medicinal Chemistry 2020, 207, 112709.

[11]. Zaręba, P.; Jaśkowska, J.; Czekaj, I.; Satała, G. Design, synthesis and molecular modelling of new bulky Fananserin derivatives with altered pharmacological profile as potential antidepressants. Bioorganic & medicinal chemistry 2019, 27, 3396-3407.

[12]. Carro, L.; Torrado, M.; Raviña, E.; Masaguer, C. F.; Lage, S.; Brea, J.; Loza, M. I. Synthesis and biological evaluation of a series of aminoalkyl-tetralones and tetralols as dual dopamine/serotonin ligands. European Journal of Medicinal Chemistry 2014, 71, 237-249.

[13]. Sun, H.; Zhu, L.; Yang, H.; Qian, W.; Guo, L.; Zhou, S.; Gao, B.; Li, Z.; Zhou, Y.; Jiang, H. Asymmetric total synthesis and identification of tetrahydroprotoberberine derivatives as new antipsychotic agents possessing a dopamine D1, D2 and serotonin 5-HT1A multi-action profile. Bioorganic & medicinal chemistry 2013, 21, 856-868.

[14]. Butini, S.; Gemma, S.; Campiani, G.; Franceschini, S.; Trotta, F.; Borriello, M.; Ceres, N.; Ros, S.; Coccone, S. S.; Bernetti, M. Discovery of a new class of potential multifunctional atypical antipsychotic agents targeting dopamine D3 and serotonin 5-HT1A and 5-HT2A receptors: design, synthesis, and effects on behavior. Journal of medicinal chemistry 2009, 52, 151-169.

[15]. Hirokawa, Y.; Fujiwara, I.; Suzuki, K.; Harada, H.; Yoshikawa, T.; Yoshida, N.; Kato, S. Synthesis and structure− affinity relationships of novel N-(1-ethyl-4-methylhexahydro-1, 4-diazepin-6-yl) pyridine-3-carboxamides with potent serotonin 5-HT3 and dopamine D2 receptor antagonistic activity. Journal of medicinal chemistry 2003, 46, 702-715.

[16]. Gómez-Jeria, J. S.; González-Ponce, N. A Quantum-chemical study of the relationships between electronic structure and affinities for the serotonin transporter protein and the 5-HT1A receptor in a series of 2H-pyrido[1,2-c]pyrimidine derivatives. Chemistry Research Journal 2020, 5, 16-31.

[17]. Gómez-Jeria, J. S.; Castro-Latorre, P.; Moreno-Rojas, C. Dissecting the drug-receptor interaction with the Klopman-Peradejordi-Gómez (KPG) method. II. The interaction of 2,5-dimethoxyphenethylamines and their N-2-methoxybenzyl-substituted analogs with 5-HT2A serotonine receptors. Chemistry Research Journal 2018, 4, 45-62.

[18]. Gómez-Jeria, J. S.; Moreno-Rojas, C. Dissecting the drug-receptor interaction with the Klopman-Peradejordi-Gómez (KPG) method. I. The interaction of 2,5-dimethoxyphenethylamines and their N-2-methoxybenzyl-substituted analogs with 5-HT1A serotonine receptors. Chemistry Research Journal 2017, 2, 27-41.

[19]. Gómez-Jeria, J. S.; Becerra-Ruiz, M. B. Electronic structure and rat fundus serotonin receptor binding affinity of phenetylamines and indolealkylamines. International Journal of Advances in Pharmacy, Biology and Chemistry 2017, 6, 72-86.

[20]. Gómez-Jeria, J. S.; Cassels, B. K.; Saavedra-Aguilar, J. C. A quantum-chemical and experimental study of the hallucinogen (±)-1-(2,5-dimethoxy-4-nitrophenyl)-2-aminopropane (DON). European Journal of Medicinal Chemistry 1987, 22, 433-437.

[21]. Gómez-Jeria, J. S.; Morales-Lagos, D.; Cassels, B. K.; Saavedra-Aguilar, J. C. Electronic structure and serotonin receptor binding affinity of 7-substituted tryptamines. Quantitative Structure-Activity Relationships 1986, 5, 153-157.

[22]. Gómez-Jeria, J. S.; Morales-Lagos, D.; Rodriguez-Gatica, J. I.; Saavedra-Aguilar, J. C. Quantum-chemical study of the relation between electronic structure and pA2 in a series of 5-substituted tryptamines. International Journal of Quantum Chemistry 1985, 28, 421-428.

[23]. Gómez-Jeria, J. S.; Morales-Lagos, D. R. Quantum chemical approach to the relationship between molecular structure and serotonin receptor binding affinity. Journal of Pharmaceutical Sciences 1984, 73, 1725-1728.

[24]. Gómez-Jeria, J. S.; López-Aravena, R. A Theoretical Analysis of the Relationships between Electronic Structure and Dopamine D4 Receptor Affinity in a series of compounds based on the classical D4 agonist A-412997. Chemistry Research Journal 2020, In press.

[25]. Gómez-Jeria, J. S.; Garrido-Sáez, N. A DFT analysis of the relationships between electronic structure and affinity for dopamine D2, D3 and D4 receptor subtypes in a group of 77-LH-28-1 derivatives. Chemistry Research Journal 2019, 4, 30-42.
[26]. Gautier, K. S.; Kpotin, G. A.; Mensah, J.-B.; Gómez-Jeria, J. S. Quantum-Chemical Study of the Relationships between Electronic Structure and the Affinity of Benzisothiazolylpiperazine Derivatives for the Dopamine Hd2l and Hd3 Receptors. The Pharmaceutical and Chemical Journal 2019, 6, 73-90.
[27]. Gómez-Jeria, J. S.; Valdebenito-Gamboa, J. A Density Functional Study of the Relationships between Electronic Structure and Dopamine D2 receptor binding affinity of a series of [4-(4-Carboxamidobutyl)]-1-arylpiperazines. Research Journal of Pharmaceutical, Biological and Chemical Sciences 2015, 6, 203-218.
[28]. Gómez-Jeria, J. S.; Valdebenito-Gamboa, J. Electronic structure and docking studies of the Dopamine D3 receptor binding affinity of a series of [4-(4-Carboxamidobutyl)]-1-arylpiperazines. Der Pharma Chemica 2015, 7, 323-347.
[29]. Gómez-Jeria, J. S.; Ojeda-Vergara, M. Electrostatic medium effects and formal quantum structure-activity relationships in apomorphines interacting with D1 and D2 dopamine receptors. International Journal of Quantum Chemistry 1997, 61, 997-1002.
[30]. Gómez Jeria, J. S. La Pharmacologie Quantique. Bollettino Chimico Farmaceutico 1982, 121, 619-625.
[31]. Gómez-Jeria, J. S. On some problems in quantum pharmacology I. The partition functions. International Journal of Quantum Chemistry 1983, 23, 1969-1972.
[32]. Gómez-Jeria, J. S. Modeling the Drug-Receptor Interaction in Quantum Pharmacology. In Molecules in Physics, Chemistry, and Biology, Maruani, J., Ed. Springer Netherlands: 1989; Vol. 4, pp 215-231.
[33]. Gómez-Jeria, J. S.; Ojeda-Vergara, M. Parametrization of the orientational effects in the drug-receptor interaction. Journal of the Chilean Chemical Society 2003, 48, 119-124.
[34]. Gómez-Jeria, J. S. Elements of Molecular Electronic Pharmacology (in Spanish). 1st ed.; Ediciones Sokar: Santiago de Chile, 2013; p 104.
[35]. Gómez-Jeria, J. S. A New Set of Local Reactivity Indices within the Hartree-Fock-Roothaan and Density Functional Theory Frameworks. Canadian Chemical Transactions 2013, 1, 25-55.
[36]. Gómez-Jeria, J. S.; Flores-Catalán, M. Quantum-chemical modeling of the relationships between molecular structure and in vitro multi-step, multimechanistic drug effects. HIV-1 replication inhibition and inhibition of cell proliferation as examples. Canadian Chemical Transactions 2013, 1, 215-237.
[37]. Paz de la Vega, A.; Alarcón, D. A.; Gómez-Jeria, J. S. Quantum Chemical Study of the Relationships between Electronic Structure and Pharmacokinetic Profile, Inhibitory Strength toward Hepatitis C virus NS5B Polymerase and HCV replicons of indole-based compounds. Journal of the Chilean Chemical Society 2013, 58, 1842-1851.
[38]. Gómez-Jeria, J. S. Tables of proposed values for the Orientational Parameter of the Substituent. I. Monoatomic, Diatomic, Triatomic, n-CnH2n+1, O-n-CnH2n+1, NRR', and Cycloalkanes (with a single ring) substituents. Research Journal of Pharmaceutical, Biological and Chemical Sciences 2016, 7, 288-294.
[39]. Gómez-Jeria, J. S. Tables of proposed values for the Orientational Parameter of the Substituent. II. Research Journal of Pharmaceutical, Biological and Chemical Sciences 2016, 7, 2258-2260.
[40]. Gómez-Jeria, J. S. 45 Years of the KPG Method: A Tribute to Federico Peradejordi. Journal of Computational Methods in Molecular Design 2017, 7, 17-37.
[41]. Gómez-Jeria, J. S.; Kpotin, G. Some Remarks on The Interpretation of The Local Atomic Reactivity Indices Within the Klopman-Peradejordi-Gómez (KPG) Method. I. Theoretical Analysis. Research Journal of Pharmaceutical, Biological and Chemical Sciences 2018, 9, 550-561.
[42]. Gómez-Jeria, J. S.; Espinoza, L. Quantum-chemical studies on acetylcholinesterasa inhibition. I. Carbamates. Journal of the Chilean Chemical Society 1982, 27, 142-144.

[43]. Gómez-Jeria, J. S.; Morales-Lagos, D. The mode of binding of phenylalkylamines to the Serotonergic Receptor. In QSAR in design of Bioactive Drugs, Kuchar, M., Ed. Prous, J.R.: Barcelona, Spain, 1984; pp 145-173.
[44]. Gómez-Jeria, J. S.; Sotomayor, P. Quantum chemical study of electronic structure and receptor binding in opiates. Journal of Molecular Structure: THEOCHEM 1988, 166, 493-498.
[45]. Gómez-Jeria, J. S.; Lagos-Arancibia, L. Quantum-chemical structure-affinity studies on kynurenic acid derivatives as Gly/NMDA receptor ligands. International Journal of Quantum Chemistry 1999, 71, 505-511.
[46]. Gómez-Jeria, J. S.; Lagos-Arancibia, L.; Sobarzo-Sánchez, E. Theoretical study of the opioid receptor selectivity of some 7-arylidenenaltrexones. Boletin de la Sociedad Chilena de Quimica 2003, 48, 61-66.
[47]. Soto-Morales, F.; Gómez-Jeria, J. S. A theoretical study of the inhibition of wild-type and drug-resistant HTV-1 reverse transcriptase by some thiazolidenebenzenesulfonamide derivatives. Journal of the Chilean Chemical Society 2007, 52, 1214-1219.
[48]. Gómez-Jeria, J. S. A DFT study of the relationships between electronic structure and peripheral benzodiazepine receptor affinity in a group of N,N-dialkyl-2- phenylindol-3-ylglyoxylamides (Erratum in: J. Chil. Chem. Soc., 55, 4, IX, 2010). Journal of the Chilean Chemical Society 2010, 55, 381-384.
[49]. Reyes-Díaz, I.; Gómez-Jeria, J. S. Quantum-chemical modeling of the hepatitis C virus replicon inhibitory potency and cytotoxicity of some pyrido[2,3-d]pyrimidine analogues. Journal of Computational Methods in Molecular Design 2013, 3, 11-21.
[50]. Gatica-Díaz, F.; Gómez-Jeria, J. S. A Theoretical Study of the Relationships between Electronic Structure and Cytotoxicity of a group of N2-alkylated Quaternary β-Carbolines against nine Tumoral Cell Lines. Journal of Computational Methods in Molecular Design 2014, 4, 79-120.
[51]. Gómez-Jeria, J. S. A quantum chemical analysis of the relationships between electronic structure, PAK1 inhibition and MEK phosphorylation in a series of 2-arylamino-4-aryl-pyrimidines. SOP Transactions on Physical Chemistry 2014, 1, 10-28.
[52]. Gómez-Jeria, J. S. Toward Understanding the Inhibition of Vesicular Stomatitis Virus Replication in MDCK Cells by 4-Quinolinecarboxylic acid Analogues. A Density Functional Study. Der Pharma Chemica 2014, 6, 64-77.
[53]. Gómez-Jeria, J. S. A DFT Study of the Inhibition of the Papain-like Protease (PLpro) from the SARS Coronavirus by a Group of 4-Piperidinecarboxamide Derivatives. Research Journal of Pharmaceutical, Biological and Chemical Sciences 2014, 5, 424-436.
[54]. Gómez-Jeria, J. S. A Density Functional Study of the Inhibition of the Anthrax Lethal Factor Toxin by Quinoline-based small Molecules related to Aminoquinuride (NSC 12155). Research Journal of Pharmaceutical, Biological and Chemical Sciences 2014, 5, 780-792.
[55]. Gómez-Jeria, J. S. A Theoretical Study of the Relationships between Electronic Structure and Antifungal Activity against Botrytis cinerea and Colletotrichum lagenarium of a Group of Carabrone Hydrazone Derivatives. Research Journal of Pharmaceutical, Biological and Chemical Sciences 2015, 6, 688-697.
[56]. Leal, M. S.; Robles-Navarro, A.; Gómez-Jeria, J. S. A Density Functional Study of the Inhibition of Microsomal Prostaglandin E2 Synthase-1 by 2-aryl substituted quinazolin-4(3H)-one, pyrido[4,3-d]pyrimidin-4(3H)-one and pyrido[2,3-d]pyrimidin-4(3H)-one derivatives. Der Pharmacia Lettre 2015, 7, 54-66.
[57]. Gómez-Jeria, J. S.; Castro-Latorre, P.; Kpotin, G. Quantum Chemical Analysis of the Relationships between Electronic Structure and Antiviral Activity against HIV-1 of some Pyrazine-1,3-thiazine Hybrid Analogues. Der Pharma Chemica 2016, 8, 234-239.
[58]. Gómez-Jeria, J. S.; Latorre-Castro, P. On the relationship between electronic structure and carcinogenic activity in substituted Benz[a]anthracene derivatives. Der Pharma Chemica 2016, 8, 84-92.

[59]. Robles-Navarro, A.; Gómez-Jeria, J. S. A Quantum-Chemical Analysis of the Relationships between Electronic Structure and Citotoxixity, GyrB inhibition, DNA Supercoiling inhibition and anti-tubercular activity of a series of quinoline–aminopiperidine hybrid analogues. Der Pharma Chemica 2016, 8, 417-440.
[60]. Gómez-Jeria, J. S.; Castro-Latorre, P. A Density Functional Theory analysis of the relationships between the Badger index measuring carcinogenicity and the electronic structure of a series of substituted Benz[a]anthracene derivatives. Chemistry Research Journal 2017, 2, 112-126.
[61]. Gómez-Jeria, J. S.; Castro-Latorre, P.; Kpotin, G. Quantum Chemical Study of the Relationships between Electronic Structure and Antiviral Activities against Influenza A H1N1, Enterovirus 71 and Coxsackie B3 viruses of some Pyrazine-1,3-thiazine Hybrid Analogues. International Journal of Research in Applied, Natural and Social Sciences 2017, 5, 49-64.
[62]. Gómez-Jeria, J. S.; Surco-Luque, J. C. A Quantum Chemical Analysis of the Relationships between Electronic Structure and the inhibition of Botulinum Neurotoxin serotype A by a series of Derivatives possessing an 8-hydroxyquinoline core. Chemistry Research Journal 2017, 2, 1-11.
[63]. Gómez-Jeria, J. S.; Moreno-Rojas, C.; Castro-Latorre, P. A note on the binding of N-2-methoxybenzyl-phenethylamines (NBOMe drugs) to the 5-HT2C receptors. Chemistry Research Journal 2018, 3, 169-175.
[64]. Abdussalam, A.; Gómez-Jeria, J. S. Quantum Chemical Study of the Relationships between Electronic Structure and Corticotropin-Releasing Factor 1 Receptor Binding Inhibition by a Group of Benzazole Derivatives. Journal of Pharmaceutical and Applied Chemistry 2019, 5, 1-9.
[65]. Gómez-Jeria, J. S.; Gatica-Díaz, N. A preliminary quantum chemical analysis of the relationships between electronic structure and 5-HT1A and 5-HT2A receptor affinity in a series of 8-acetyl-7-hydroxy-4-methylcoumarin derivatives. Chemistry Research Journal 2019, 4, 85-100.
[66]. Gómez-Jeria, J. S.; Soloaga Ardiles, C. E.; Kpotin, G. A. A DFT Analysis of the Relationships between Electronic Structure and Human κ, δ and μ Opioid Receptor Binding Affinity in a series of Diphenethylamines. Chemistry Research Journal 2020, 5, 32-46.
[67]. Gómez-Jeria, J. S.; Valenzuela-Hueichaqueo, N. J. The relationships between electronic structure and human A1 adenosine receptor binding affinity in a series of triazolopyridine derivatives. Chemistry Research Journal 2020, 5, 226-236.
[68]. The results presented here are obtained from what is now a routinary procedure. For this reason, we built a general model for the paper's structure. This model contains standard phrases for the presentation of the methods, calculations and results because they do not need to be rewritten repeatedly and the number of possible variations to use is finite. In.
[69]. Frisch, M. J.; Trucks, G. W.; Schlegel, H. B.; Scuseria, G. E.; Robb, M. A.; Cheeseman, J. R.; Montgomery, J., J.A.; Vreven, T.; Kudin, K. N.; Burant, J. C.; Millam, J. M.; Iyengar, S. S.; Tomasi, J.; Barone, V.; Mennucci, B.; Cossi, M.; Scalmani, G.; Rega, N. G03 Rev. E.01, Gaussian: Pittsburgh, PA, USA, 2007.
[70]. Gómez-Jeria, J. S. D-Cent-QSAR: A program to generate Local Atomic Reactivity Indices from Gaussian 03 log files. v. 1.0, v. 1.0; Santiago, Chile, 2014.
[71]. Gómez-Jeria, J. S. An empirical way to correct some drawbacks of Mulliken Population Analysis (Erratum in: J. Chil. Chem. Soc., 55, 4, IX, 2010). Journal of the Chilean Chemical Society 2009, 54, 482-485.
[72]. Statsoft. Statistica v. 8.0, 2300 East 14 th St. Tulsa, OK 74104, USA, 1984-2007.
[73]. Gómez-Jeria, J. S.; Robles-Navarro, A.; Kpotin, G. A.; Garrido-Sáez, N.; Gatica-Díaz, N. Some remarks about the relationships between the common skeleton concept within the Klopman-Peradejordi-Gómez QSAR method and the weak molecule-site interactions. Chemistry Research Journal 2020, 5, 32-52.